

Nanoporous Structured Submicrometer Carbon Fibers Prepared via Solution Electrospinning of Polymer Blends

Mao Peng,* Dasong Li, Lie Shen,* Ying Chen, Qiang Zheng, and Huijun Wang

Department of Polymer Science & Engineering, Zhejiang University, Hangzhou, 310027, China

Received April 28, 2006. In Final Form: September 1, 2006

A facile means for obtaining submicrometer carbon fibers with a nanoporous structure is presented. A mixture of polyacrylonitrile (PAN) and a copolymer of acrylonitrile and methyl methacrylate (poly(AN-co-MMA)) in dimethylformamide was electrospun into submicrometer fibers with a microphase-separated structure. During the followed oxidation process, the copolymer domains were pyrolyzed, resulting in a nanoporous structure that was preserved after carbonization. The microphase-separated structure of the PAN/poly(AN-co-MMA) electrospun fibers, the morphology, and porous structure of both the oxidized and the carbonized fibers were observed with scanning electron microscopy and transmission electron microscopy. The carbon fibers have diameters ranging from several hundred nanometers to about 1 μm . The nanopores or nanoslits throughout the fiber surface and interior with diameters of several tens of nanometers are interconnected and oriented along the longitudinal axis of the fibers. This unique nanoporous morphology similar to the microphase-separated structure in the PAN/poly(AN-co-MMA) fibers is attributed to the rapid phase separation, solidification, as well as the stretching of the fibers during electrospinning. The pore volume and pore size distribution of the carbonized fibers were investigated by nitrogen adsorption and desorption.

Introduction

Porous carbonaceous materials have been widely used in adsorption-related industrial processes such as gas storage, separation, and purification, or as catalyst carriers, electrode materials for cells, and electrochemical double-layer supercapacitors, because of their unique mechanical properties, heat resistance, chemical inertness, etc.^{1–5} Porous materials are classified as microporous (pore dimensions < 2 nm), mesoporous (2–50 nm), and macroporous (> 50 nm). Both pore size and morphology play important roles in determining the final properties of porous carbon. Mesoporous/macroporous carbon is often made on templated materials, mesoporous silica with an ordered structure being a representing example.^{6–10} Well-defined pores can be created by removal of silica with hydrofluoric acid or concentrated alkali. Block copolymers¹¹ and polymer colloids obtained by microemulsion polymerization¹² can also be used as templated materials. Pyrolysis of one component of the block copolymers or the polymer colloids results in a porous structure. Phase-separated polymer blends of poly(ethylene glycol) (PEG) and polyimide (PI)¹³ can be made into mesoporous carbon membranes by pyrolysis of PEG and carbonization of PI.

Recently, preparation of ultrathin fibers by electrospinning polymer solutions or melts has arrested many efforts. During electrospinning, a strong electrostatic field is applied to the spinneret from which a polymer solution is extruded. When the electrostatic force is strong enough to overcome the surface tension of the solution, the droplet becomes conical (Taylor cone) and then ejects from the spinneret. Nonwoven fabrics made of ultrathin fibers with diameters from several tens of nanometers up to several micrometers are obtained on the grounded metal electrode placed opposite to the spinneret. In contrast, the conventional solution and/or melt spinning can only prepare fibers with diameters in the order of several or several tens of micrometers. Therefore, ultrathin electrospun fibers/fabrics are now believed to be ideal candidates for new generation of filtration materials, carriers for catalysts, enzymes and drugs, etc. Up to date, electrospun fibers of a variety of polymers, metal oxides, and, more recently, composite fibers with embedded carbon nanotubes^{14–16} or nanoparticles^{17,18} have been successfully created. Pitch-based carbon fibers or activated carbon fibers¹⁹ and PAN-based carbon fibers embedded with carbon nanotubes²⁰ were also prepared by electrospinning.

At the same time, not only the control of fiber diameters but also the morphology of some highly structured fibers is being paid more and more attention. There have been a few reports on the preparation of porous electrospun fibers with submicrometer or nanosized pores. Wendorff et al.²¹ found that when spinning

* Corresponding author. Phone: ++86-571-87953075. Fax: ++86-571-87952522. E-mail: pengmao@zju.edu.cn (M.P.); shenlie@zju.edu.cn (L.S.).

(1) Zhao, X. B.; Xiao, B.; Fletcher, A. J.; Thomas, K. M. *J. Phys. Chem. B* **2005**, *109*, 8880.

(2) Lozano-Castello, D.; Cazorla-Amoros, D.; Linares-Solano, A. *Energy Fuels* **2002**, *16*, 1321.

(3) Polarz, S.; Smarsly, B.; Schattka, J. H. *Chem. Mater.* **2002**, *14*, 2940.

(4) Kadirvelu, K.; Faur-Brasquet, C.; Cloirec, P. L. *Langmuir* **2000**, *16*, 8404.

(5) Villar-Rodil, S.; Suarez-Garcia, F.; Paredes, J. I.; Martinez-Alonso, A.; Tascon, J. M. D. *Chem. Mater.* **2005**, *17*, 5893.

(6) Kawashima, D.; Aihara, T.; Kobayashi, Y.; Kyotani, T.; Tomita, A. *Chem. Mater.* **2000**, *12*, 3397.

(7) Kruk, M.; Dufour, B.; Celer, E. B.; Kowalewski, T.; Jaroniec, M.; Matyjaszewski, K. *Chem. Mater.* **2006**, *18*, 1417.

(8) Han, S. J.; Lee, K. T.; Oh, S. M.; Hyeon, T. W. *Carbon* **2003**, *41*, 1049.

(9) Lee, G. J.; Pyun, S. I. *Carbon* **2005**, *43*, 1804.

(10) Kruk, M.; Dufour, B.; Celer, E. B.; Kowalewski, T.; Jaroniec, M.; Matyjaszewski, K. *J. Phys. Chem. B* **2005**, *109*, 9216.

(11) Liang, C. D.; Hong, K. L.; Guiochon, G. A.; Mays, J. W.; Dai, S. *Angew. Chem.* **2004**, *116*, 5909.

(12) (a) Lukens, W. W.; Stucky, G. D. *Chem. Mater.* **2002**, *14*, 1665. (b) Wang, Z. Y.; Ergang, N. S.; Al-Daous, M. A.; Stein, A. *Chem. Mater.* **2005**, *17*, 6805.

(13) Hatori, H.; Kobayashi, T.; Hanzawa, Y.; Yamada, Y.; Limura, Y.; Kimura, T.; Shiraishi, M. *J. Appl. Polym. Sci.* **2001**, *79*, 836.

(14) Salalha, W.; Dror, Y.; Khalfin, R. L.; Cohen, Y.; Yarin, A. L.; Zussman, E. *Langmuir* **2004**, *20*, 9852.

(15) Hou, H.; Ge, J. J.; Zeng, J.; Li, Q.; Reneker, D. H.; Greiner, A.; Cheng, S. Z. D. *Chem. Mater.* **2005**, *17*, 967.

(16) Dror, Y.; Salalha, W.; Khalfin, R. L.; Cohen, Y.; Yarin, A. L.; Zussman, E. *Langmuir* **2003**, *19*, 7012.

(17) Ji, Y.; Li, B.; Ge, S.; Sokolov, J. C.; Rafailovich, M. H. *Langmuir* **2006**, *22*, 1321.

(18) Kedem, S.; Schmidt, J.; Paz, Y.; Cohen, Y. *Langmuir* **2005**, *21*, 5600.

(19) Park, S. H.; Kim, C.; Choi, Y. O.; Yang, K. S. *Carbon* **2003**, *41*, 2655.

(20) Chakrabarti, K.; Nambissan, P. M. G.; Mukherjee, C. D.; Bardhan, K. K.; Kim, C.; Yang, K. S. *Carbon* **2006**, *44*, 948.

(21) Bognitzki, M.; Czado, W.; Frese, T.; Schaper, A.; Hellwig, M.; Steinhart, M.; Greiner, A.; Wendorff, J. H. *Adv. Mater.* **2001**, *13*, 70.

parameters and highly volatile solvents were chosen appropriately, porous electrospun fibers are obtained. Rabolt et al.²² investigated in detail the influence of volatile solvents on the surface morphology of polymer electrospun fibers. Because of evaporative cooling during electrospinning, the atmospheric water vapor condensed onto the fiber surface formed droplets leading to a porous surface fiber. Densely packed nanopores located only on the fiber surface were observed. Polylactide (PLA) or poly(vinylpyrrolidone) (PVP) porous fibers have been prepared by electrospinning a dichloromethane (DCM) solution of a mixture of PLA and PVP followed by selectively removing one of the two components from the fibers.²³ The fibers have diameters of about 1–3 μm with a co-continuous porous structure and pore size of about 100 nm. Whether PLA or PVP is the major component, the fibers remain compact with a core-sheath structure. Balkus et al.²⁴ prepared mesoporous molecular sieve fibers with diameters of a few hundred nanometers or about 1 μm by electrospinning a solution of tetraethoxysilane (TEOS) or tetramethoxysilane (TMOS) in a mixture of water and ethanol. In the process, various surfactants were used as structure-directing agents. Xia et al.²⁵ prepared nanofibers with a core-sheath structure by electrospinning with a coaxial spinneret. Porous titania (TiO_2) submicrometer fibers could be obtained when a solution of polystyrene in a mixture of dimethylformamide (DMF) and tetrahydrofuran (THF) was spun from the core capillary while TiO_2 -PVP was spun from the sheath capillary. More recently, Xia and his coauthors²⁶ reported that, by immersing the collector in a bath of liquid nitrogen during electrospinning, highly porous fibers of polystyrene, poly(vinylidene fluoride), poly(ϵ -caprolactone), and PAN were successfully obtained through thermally induced phase separation between the solvent-rich and solvent-poor regions in the fiber. Porous carbon fibers could be obtained by carbonization of the porous PAN fibers. Up to date, it has been well accepted that electrospun fibers with nanosized porous structure have much larger surface area-to-volume ratios and, therefore, are of interest for many applications. It is also reasonable to expect that submicrometer porous carbonaceous fibers will find a great many applications in the future. However, to our knowledge, the investigation of the preparation of porous carbon fibers by electrospinning is still rare.

In this study, we report a novel strategy for preparing ultrathin nanoporous carbon fibers through electrospinning. A binary mixture of PAN and poly(AN-co-MMA) in DMF was electrospun into submicrometer fibers. During electrospinning, the two polymers became incompatible with DMF evaporating, and phase separation occurred leading to microphase-separation structured fibers. After oxidation and carbonization, the copolymer domains were pyrolyzed, and the residual carbon fibers had an interconnected nanopore network with dimensions of several tens of nanometers throughout the surface and the interior. The morphology of the nanoporous carbon fibers was observed with field emission scanning electron microscopy (FE-SEM) and transmission electron microscopy (TEM). The nitrogen adsorption/desorption isotherms were employed to measure the pore volume, pore size distribution, and specific surface area. The morphology and domain size of the electrospun fibers were compared to those of a spin-casting film, and pyrolysis behavior

of the electrospun fibers was investigated with thermal gravimetric analysis (TGA).

Experimental Section

Materials. Monomers AN and MMA, initiator potassium persulfate (KPS), solvents DMF and DCM, and PVP were purchased from China Medicine (Group) Shanghai Chemical Reagent Corp. (Shanghai, China) and were used without further purification. PAN and poly(AN-co-MMA) were synthesized by free radical polymerization in water at 70 $^\circ\text{C}$ using KPS as initiator and PVP as stabilizer. The molar ratio of AN to MMA in the copolymer was 1:9. The KPS and PVP concentrations were 0.2 and 0.1 wt % to the monomers, respectively. The overall conversions of polymerization were determined to be 90.6 and 84.5 wt %, respectively, for PAN and the copolymer. The polymers were dried in a vacuum at 60 $^\circ\text{C}$ for overnight and washed by a large amount of alcohol to remove possible residual monomer and initiator. PAN and poly(AN-co-MMA) were then dissolved in DMF with a ratio of 40:60 (w/w). The total concentration of the polymers in DMF was 3 wt %.

Phase Contrast Microscope (PCM) Observation. A DMF solution of a mixture of PAN and poly(AN-co-MMA) (40:60 by weight) was dropped onto a glass slide and spin-cast at 3000 rpm. The thickness of the sample film was in the order of several micrometers. The sample film was then dried under ambient environment for more than 48 h. As DMF evaporates slowly at room temperature, the sample film becomes opaque gradually. The phase structure of the spin-coated film was observed with a PCM (Motic BI-220PH, Motic China, Xiamen, China), and the image was recorded with a digital camera (Nikon Coolpix4500) with a resolution of 1.9 megapixels.

Preparation of Porous Carbon Fibers. Some PAN and poly(AN-co-MMA) powders were weighed and added into DMF. The suspension was stirred fiercely with a magnetic stirrer until the polymers were completely dissolved. Electrospinning was conducted with an apparatus similar to that reported in the literature.²² The polymer solution was placed into a 50 mL syringe attached to a syringe pump in a vertical mount. The potential was applied to the tip of the needle using a high voltage power supplier (Qiaofeng Electrostatic Equipment Factory, Hangzhou, China). Electrospinning was conducted using a voltage of 30 kV and an extrusion rate of 1.0 mL/h under ambient condition. The fibers were collected on the grounded aluminum foil placed on the surface of an adjustable lab jack as the target. The distance between the target and the tip of the needle was 12 cm. After electrospinning, the obtained fabrics were further dried at 80 $^\circ\text{C}$ in a vacuum oven overnight. In previous studies, carbon fibers or porous carbon from PAN are ordinarily prepared through the following two steps: (a) oxidative stabilization in air at a temperature between 200 and 300 $^\circ\text{C}$,^{27,28} and (b) final carbonization in an inert atmosphere at temperatures between 800 and 3000 $^\circ\text{C}$ for carbon fibers²⁷ or between 600 and 1000 $^\circ\text{C}$ for porous carbon.²⁸ So the following treatment was performed to obtain porous carbon fibers in this study: the pristine fabrics were heated to about 260–300 $^\circ\text{C}$ in a muffle and held there for 2 h. They turned from white to dark brown in color. Next, the oxidized samples were placed into a quartz tube housed within an electric tube furnace. Under the protection of nitrogen, the samples were gradually heated to 800 $^\circ\text{C}$ over 4 h and then held for half an hour at 800 $^\circ\text{C}$ for carbonization.

TGA Measurement. To understand the formation of porous structure in electrospun fibers, a Pyris 1 Thermal Gravimetric Analyzer (Perkin-Elmer, USA) was used to determine the weight loss of the electrospun fibers of PAN, poly(AN-co-MMA), and their blends under the oxidizing condition (280 $^\circ\text{C}$ in air). Furthermore,

(22) (a) Megelski, S.; Stephens, J. S.; Chase, D. B.; Rabolt, J. F. *Macromolecules* **2002**, *35*, 8456. (b) Casper, C. L.; Stephens, J. S.; Tassi, N. G.; Chase, D. B.; Rabolt, J. F. *Macromolecules* **2004**, *37*, 573.

(23) Bognitzki, M.; Frese, T.; Steinhart, M.; Greiner, A.; Wendorff, J. H. *Polym. Eng. Sci.* **2001**, *41*, 982.

(24) Madhugiri, S.; Dalton, A.; Gutierrez, J.; Ferraris, J. P.; Balkus, K. J. *J. Am. Chem. Soc.* **2003**, *125*, 14531.

(25) Li, D.; Xia, Y. *Nano Lett.* **2004**, *4*, 933.

(26) McCann, J. T.; Marquez, M.; Xia, Y. *J. Am. Chem. Soc.* **2006**, *128*, 1436.

(27) (a) Chen, J. C.; Harrison, I. R. *Carbon* **2002**, *40*, 25. (b) Edie, D. D. *Carbon* **1998**, *36*, 345. (c) Fennessey, S. F.; Farris, R. J. *Polymer* **2004**, *45*, 4217. (d) Dalton, S.; Heatley, F.; Budd, P. M. *Polymer* **1999**, *40*, 5531. (e) Rizzo, P.; Guerra, G.; Aurimemma, F. *Macromolecules* **1996**, *29*, 1830.

(28) (a) Kruk, M.; Dufour, B.; Celer, E. B.; Kowalewski, T.; Jaroniec, M.; Matyjaszewski, K. *Chem. Mater.* **2006**, *18*, 1417. (b) Kowalewski, T.; Tsarevsky, N. V.; Matyjaszewski, K. *J. Am. Chem. Soc.* **2002**, *124*, 10632. (c) Leiston-Belanger, J. M.; Penelle, J.; Russell, T. P. *Macromolecules* **2006**, *39*, 1766.

the pyrolysis behavior of the as-electrospun fibers, oxidized fibers, and carbonized fibers were investigated by heating the samples to 900 °C at a rate of 20 °C min⁻¹ under nitrogen protection.

Characterization of Materials. FE-SEM and TEM were used to observe the microphase-separated structure of the PAN/poly(AN-*co*-MMA) electrospun fibers. An appropriate amount of electrospun fibers was placed into DCM and soaked for more than 12 h to selectively remove the soluble copolymer phase. The residual fibers were dried and sputter-coated with gold and then observed on a SIRION FE-SEM (FEI, The Netherlands). The rinsed fibers were dispersed in ethanol, and the suspension was deposited on cellulose acetate-coated copper grids for TEM observation, which was performed with a JEOL-1230 (JEOL, Japan) at a voltage of 120 kV.

The morphologies of oxidized and carbonized fibers were also observed by using the same FE-SEM apparatus. TEM observation for the carbonized fibers was performed using a JEOL-2000EX (JEOL, Japan) microscope operated at a voltage of 120 kV. The carbonized fibers were embedded in the melts of PMMA at 170 °C and then cooled off. Thin sample films with a thickness of about 200 nm were prepared using a Power Tome PC ultramicrotome (RMC, USA) for TEM observation. The samples were cut parallel and vertically to the axis of the carbon fibers, respectively, to observe both the cross-section and the longitudinal section morphologies.

Nitrogen adsorption and desorption isotherms of the carbonized electrospun fibers at 77.35 K were recorded using an Autosorb-1-C volumetric adsorption analyzer (Quantachrome Instruments, USA) after the sample was degassed at 473 K for 2 h in a vacuum. The specific surface area was obtained over a relative pressure (P/P_0) range of 0.003–0.081 using the Brunauer–Emmett–Teller (BET) method. The pore size distribution was calculated using the Brunauer–Joyner–Hallenda (BJH) method.

Results

Compatibility of PAN and Poly(AN-*co*-MMA). A copolymer of AN and MMA instead of the homopolymer of MMA (PMMA) has been employed as the second component in the polymer mixture for the purpose of improving the compatibility of the second component with PAN in DMF, and so the stability of the solution during electrospinning. We found that PAN and poly(MMA-*co*-AN) formed a transparent and uniform solution in DMF when the total polymer content was below 15 wt %, regardless of the PAN/copolymer ratio. The solution in the syringe remained stable during electrospinning. On the contrary, when PMMA was used as the second component, it was observed that during electrospinning the blend solution in the syringe tended to become two layers, indicating an occurrence of apparent phase separation in the solution.

As aforementioned, the PAN/poly(AN-*co*-MMA) mixture became immiscible, and an evident phase separation occurred with the evaporation of DMF. The phase-separated morphology of a spin-casting PAN/poly(MMA-*co*-AN) film was observed using PCM as shown in Figure 1. An interconnected phase-separated morphology can be observed. The average domain size of the sample is about 2 μm. The phase separation process of a binary polymer mixture in a solvent is rather complex, because during solvent evaporation not only the solvent becomes incompatible with the polymers but also the two polymers become incompatible. Moreover, because PAN is a semicrystalline polymer, both liquid–liquid phase separation and crystallization occur with DMF evaporating, further adding to the complexity of the phase separation behavior. Thus, a complete description of this process is still very difficult. Yet, at least one thing can be sure, that the bicontinuous, that is, interconnected morphology in Figure 1, which can be frequently observed in polymer mixtures undergoing spinodal decomposition (SD), suggests a SD mechanism for the phase separation of the PAN/poly(MMA-*co*-AN)/

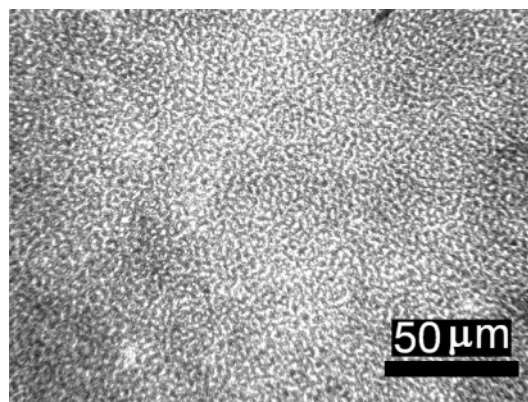


Figure 1. Phase contrast microscope (PCM) image of the spin-cast film of PAN/poly(AN-*co*-MMA) blends showing an interconnected phase-separated structure with an average domain size of about 2 μm.

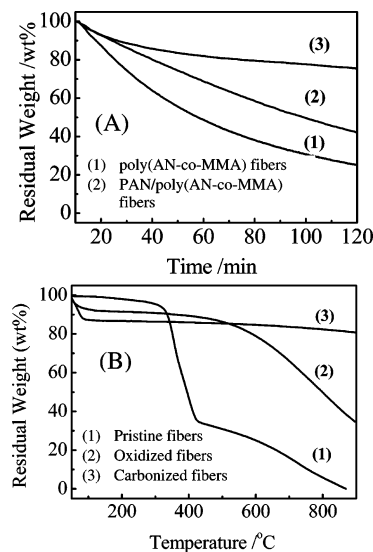


Figure 2. (A) TGA analysis in the isothermal mode for the poly(AN-*co*-MMA) electrospun fibers (1), PAN/poly(AN-*co*-MMA) fibers (2), and PAN fibers (3), respectively; (B) TGA curves at a heating rate of 20 °C/min for the pristine (1), the oxidized (2), and the carbonized fibers (3), respectively.

DMF solution. Because the DMF solution of PAN/poly(AN-*co*-MMA) is stable and it separates into two phases as a result of DMF evaporation, it is reasonable to speculate that ultrathin fibers with phase-separated structures can be obtained by electrospinning.

TGA Thermograms. The chemistry of oxidative stabilization and carbonization of PAN has been studied extensively due to its importance as a precursor for carbon fibers or porous carbon. It has been shown that, before being carbonized under the protection of inert gases, PAN fibers must be stabilized in an oxidizing atmosphere (e.g., air in most cases) sufficiently to prevent melting or fusion of the fiber and avoid excessive volatilization of elemental carbon in the carbonization step. To better understand the pyrolysis behavior and mechanism of nanopores formation during the oxidation and carbonization processes of the electrospun fibers, TGA experiments in the isothermal mode were conducted for the electrospun fibers of PAN, poly(AN-*co*-MMA), and their blends at 280 °C under a dry airflow as shown in Figure 2A. The weight loss of pure PAN fibers is rapid at the beginning but levels off gradually until approaching 24.3 wt % (curve 3). According to previous

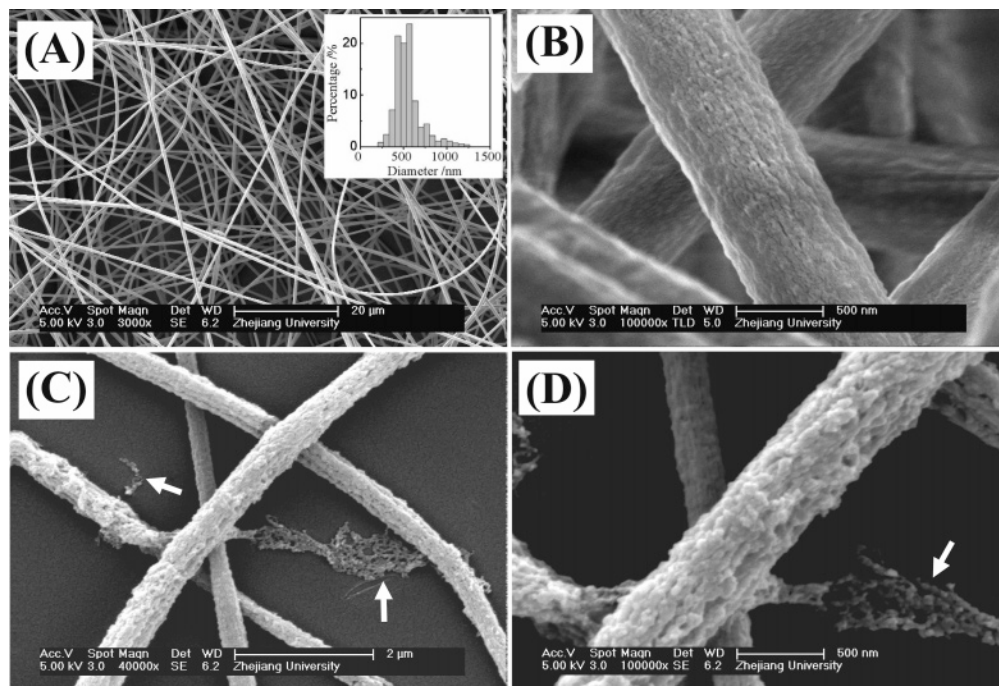


Figure 3. Field emission scanning electron microscope (FE-SEM) images of the electrospun fibers at magnifications of 3000 \times (A) and 10 000 \times (B), respectively, and FE-SEM images of the DCM rinsed electrospun fibers at magnifications of 40 000 \times (C) and 100 000 \times (D), respectively. The inset in (A) presents the diameter distribution determined from SEM images.

studies,^{27,29} such weight loss results from releases of volatile small molecular weight fragments, accompanied by chain scissions, dehydrogenations, and cyclization reactions of the nitrile groups into an extended conjugated ring system. Thermally stable aromatic ladder polymers form after this process. As to the copolymer fibers, the weight loss is 74.3 wt % after 2 h exposure at 280 °C (curve 1), which is about 3 times that of pure PAN fibers. Obviously, degradation of MMA segments in the copolymer contributes to this excessive weight loss, because PMMA degradation occurs at temperatures above 220 °C in air.³⁰ The blended PAN/poly(AN-*co*-MMA) (40:60) fibers exhibit a weight loss of about 42.6 wt % (curve 2), which is between those of PAN and poly(AN-*co*-MMA) fibers. Therefore, it is reasonable to suppose that when thermal oxidation is performed on PAN/poly(AN-*co*-MMA) blends with a phase-separated structure, the weight loss of PAN-rich domains will be much less than that of copolymer-rich domains, which may result in a porous structure. This will be validated by the SEM observation in the following section.

Thermogravimetric analysis at a heating rate of 20 °C/min was further performed on the pristine electrospun fibers, the oxidized fibers, and the carbonized fibers, respectively, as shown in Figure 2B. For the pristine fibers (curve 1), rapid weight loss occurs at temperatures above 300 °C and the residual weight is about 35.0 wt % at 420 °C, which is somewhat smaller than the PAN content in the mixture. After that, the weight loss becomes much slower. This indicates that the abrupt weight loss between 300 and 420 °C mainly results from the pyrolysis of MMA segments in the copolymer domains. For the oxidized fibers (curve 2), about 7.5 wt % weight loss can be observed when the temperature increases from 50 to about 100 °C. This phenomenon should result from the evaporation of water adsorbed in the

oxidized fibers (i.e., capillary condensation), which also offers an evidence for the existence of a porous structure in the fibers. The weight loss becomes faster at temperatures above 450 °C. As there is almost no observable weight loss between 300 and 400 °C, it is reasonable to believe that the MMA segments in the copolymer domains have been almost completely pyrolyzed during oxidation. As to the carbonized fibers (curve 3), about 13.0 wt % weight loss is observed at temperatures between 50 and 110 °C, which also implies the existence of a porous structure in the carbonized fibers. At higher temperatures, the sample weight decreases only slightly with increasing temperature.

Microstructure of the Electrospun PAN/Poly(AN-*co*-MMA) Fibers. It is well known that electrospinning is influenced by many factors, such as the applied voltage, solution feeding rate, distance between the tip of needle and the collector, as well as solution properties including concentration, viscosity, viscoelasticity, conductivity, etc. As mentioned above, the DMF solution of PAN/poly(MMA-*co*-AN) exhibited good electrospinnability under the experimental conditions. Both optical and FE-SEM (Figure 3A) observations indicate that the as-spun fibers are solid and uniform in both shape and size. Defects frequently observed in electrospun fibers, such as beads or fibers with the so-called “beads on a string” morphology, are seldom observed in our samples, indicating that the sample solution used in this study is appropriate for electrospinning. The inset in Figure 3A shows the diameter distribution of the electrospun fibers, determined from SEM images. The fiber diameters range from about 200 nm to 1.2 μ m with a mean diameter of about 500 nm. Furthermore, the zoom-in SEM image in Figure 3B shows that the fibers are solid and have a slightly rough surface. According to previous studies,²² electrospun fibers with micro- and nanostructured surfaces were directly obtained when the solvents used were highly volatile, and with the decrease of volatility, the fiber surface became less porous. This explains the nonporous morphology of the as-electrospun fibers obtained in this study, because DMF is a kind of solvent with a high boiling point (153 °C) and a low vapor pressure (2.7 kPa at room temperature).

(29) (a) Usami, T.; Itoh, T.; Ohtani, H.; Tsuge, S. *Macromolecules* **1990**, *23*, 2460. (b) Giunta, P. R.; van de Burgt, L. J.; Stieglman, A. E. *Chem. Mater.* **2005**, *7*, 1234.

(30) (a) Aymonier, C.; Bortzmeyer, D.; Thomann, R.; Mulhaupt, R. *Chem. Mater.* **2003**, *15*, 4874. (b) Monleon Pradas, M.; Schaber, G.; Gomez Ribelles, J. L.; Romero Colomer, F. *Macromolecules* **1997**, *30*, 3612.

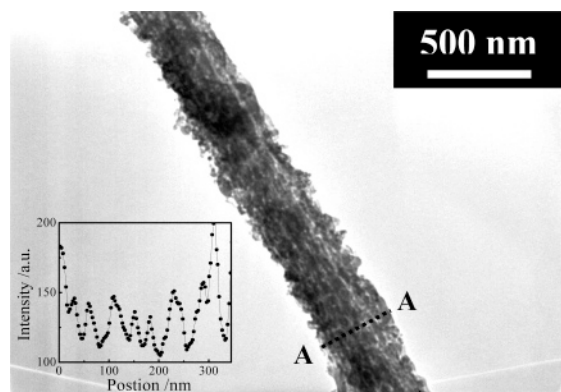


Figure 4. TEM image of the DCM rinsed PAN/poly(AN-*co*-MMA) (40:60) fibers.

The microphase-separated structure of the electrospun fibers was explored by selectively removing the copolymer-rich domains by rinsing the electrospun fibers in DCM, because poly(AN-*co*-MMA) is soluble in DCM while PAN is completely insoluble. Figure 3C and D sheds light on the morphology of the residual fibers that have phase-separation induced structure. Obviously, after the copolymer domains were selectively removed, most of the residual fibers keep continuous and their morphology and size are similar to those of fibers before being rinsed. Some of the fibers are seriously distorted, leaving highly porous residues as denoted with white arrows. Yet, fortunately, this distortion is infrequently observed. So, it is certain that the composition and phase structure are rather uniform for most of the electrospun fibers. More important, in comparison with the as-spun fibers in Figure 3B, the surface topology of the rinsed fibers is rather rough with a large amount of nodules, pores, and pits. The pores and pits are apparently elongated along the longitudinal axis of the fibers, and their sizes are of several tens of nanometers.

The interior morphology is observed for the DCM etched electrospun fibers with TEM as shown in Figure 4. The fibers are not thin enough, and therefore it is difficult to obtain clear images uncovering the interior morphology of the fibers through TEM observations. However, elongated narrow pores spreading throughout the interior of the fibers can still be viewed. Also, the surface of the fibers is rather rough. The inset of Figure 4 presents the intensity profile along the A–A line on the fiber, which is vertical to the longitudinal axis of the fiber. A periodic increase and decrease of the intensity indicates the existence of a periodic structure within the fiber. The pore and domain size can be evaluated as half of the periodic distance between two neighboring intensity peaks. Therefore, the average diameters of the pores and phase domains are about 20 nm, which is similar to the size of the pores on the fiber surface.

In general, both the FE-SEM and the TEM observations indicate that the electrospun fibers from the DMF solution of the mixture of PAN and poly(AN-*co*-MMA) have a microphase-separated structure with an average domain size of several tens of nanometers. The rapid solvent evaporation and fiber solidification during electrospinning cannot completely suppress the occurrence of phase separation between PAN and poly(AN-*co*-MMA). Meanwhile, the fact that the copolymer phase domains inside the fiber can be simply removed by soaking statically in DCM suggests that the copolymer domains in the fibers are continuous.

Characterization of the Oxidized and the Carbonized Fibers. It is important to trace the morphology changes and the porous structure formation in the fibers during the oxidation and the carbonization procedures. The electrospun fabrics turned from white to dark brown after oxidation, and, more interestingly,

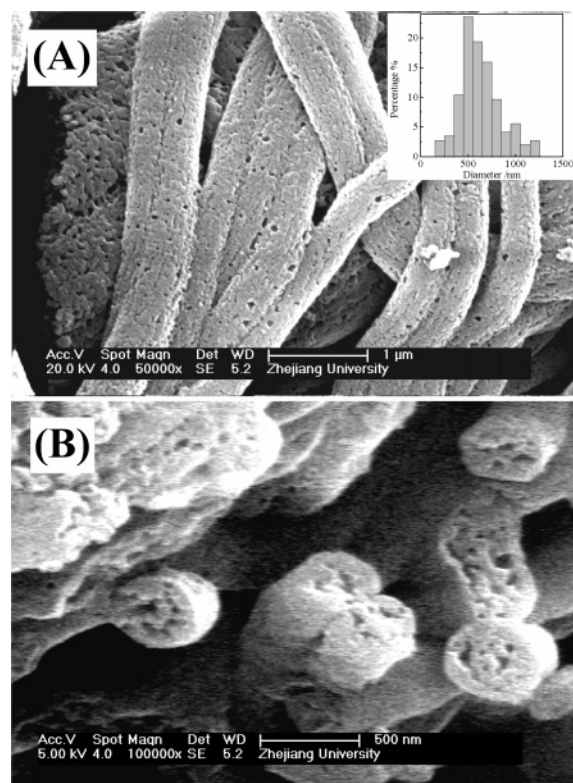


Figure 5. FE-SEM images of the side surface (A) and the cross-section (B) of the oxidized fibers.

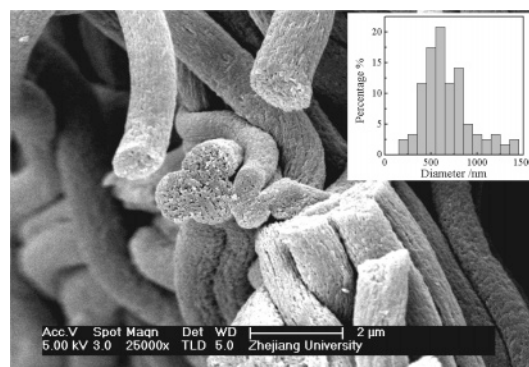


Figure 6. FE-SEM image of the carbonized fibers.

they shrank dramatically. From the FE-SEM images in Figure 5, one can find that the oxidized fibers stack much more closely in contrast to the as-spun PAN/poly(AN-*co*-MMA) fibers in Figure 3A. The fiber diameters are similar to those of as-spun fibers, with an average diameter of about 500 nm. More important, obvious porous structures are observed on both the surface and the cross-section of the oxidized electrospun fibers. The pore shape as well as pore size ranging from 20 to 70 nm are also similar to those of the phase domains observed in DCM etched PAN/poly(AN-*co*-MMA) fibers. This result directly confirms our speculation that it is during the oxidation procedure that the porous structure forms in the fibers as the result of degradation and pyrolysis of the copolymer domains and also indicates that the PAN-rich domains are stiff enough to prevent the closing up of pores during oxidation.

Figure 6 shows the FE-SEM image of the carbonized fibers. After carbonization, the samples remain fibrous. Similar to the oxidized fibers, obvious porous morphology can be observed on both the surface and the cross-section of the carbonized fibers. The inset shows the diameter distribution of carbonized fibers with a mean diameter of about 600 nm, which is somewhat

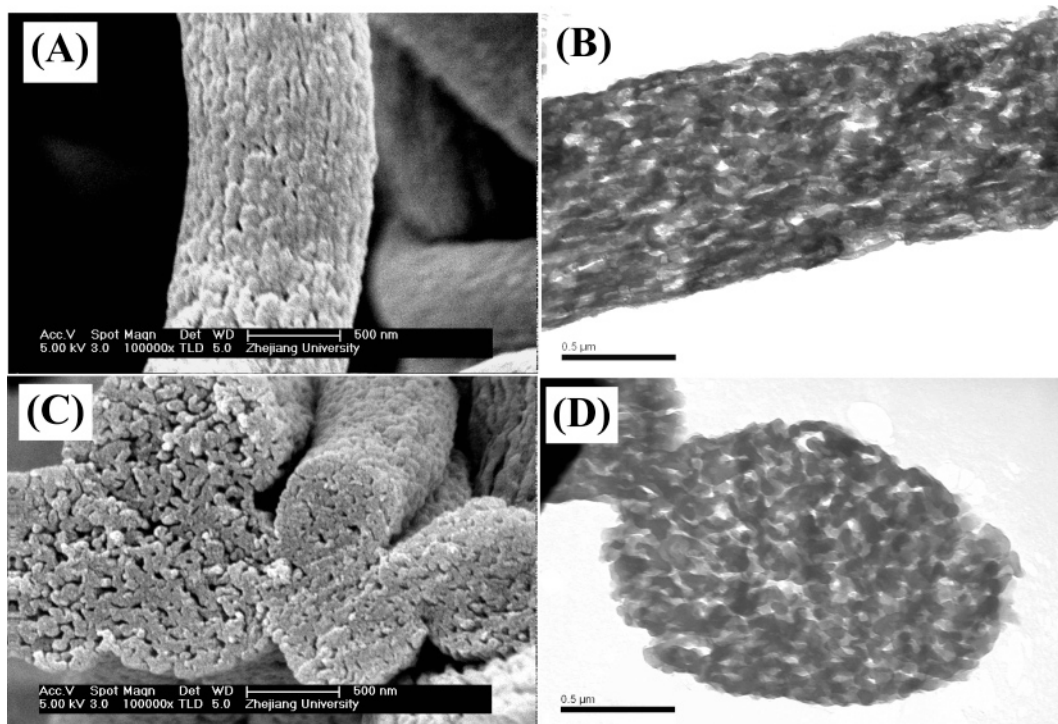


Figure 7. (A) FE-SEM image of the side surface of the porous carbon fiber with oriented pores. (B) TEM image of the longitudinal section of the porous carbon fiber. (C) FE-SEM image of the cross-section of the carbon fibers. (D) TEM image of the cross-section of the carbon fibers.

larger than that of the pristine electrospun fibers and the oxidized fibers. A further detailed surface morphology of the carbonized fibers in Figure 7A shows some narrow and elongated nanopores or slits with widths of about 20–40 nm. The pores in the fiber are also elongated longitudinally (Figure 7B), and, more important, the pores and the carbon domains seem to be interconnected, indicating a co-continuous internal phase structure of the fibers. As to the cross-section morphology of the fibers, both FE-SEM and TEM images reveal an evident spongelike structure; that is, the wormlike carbon domains and the pores are interconnected and form networks (Figure 7C,D). The width of the pores is about 20–60 nm, which is somewhat larger than that of pores on fiber surface, and the carbon domains are about 30–100 nm. It affirms that the pores remain the same in morphology after carbonization. It is worthy to note that this wormlike interconnected structure is widely observed in the early or intermediate stage of SD of many binary polymer blends.

The nitrogen adsorption and desorption isotherms in Figure 8 exhibit an obvious hysteresis loop over a wide range of relative pressure (P/P_0); that is, the desorption branch lies above the adsorption branch. This feature is typical of mesoporous materials exhibiting the capillary condensation/evaporation behavior. The hysteresis loop belongs to the H4 type according to the classification of IUPAC, which is often associated with narrow slitlike mesopores. Yet, it should be noted that the hysteresis loop is extremely broad (from P/P_0 of 0.012 to 0.991), as compared to those reported in the literature. This indicates the heterogeneity in the size and shape of pores in the carbonized electrospun fibers. This should originate from the labyrinth morphology of the interconnected pores with inhomogeneous pore size and shape inside the fibers, as we have observed in the SEM and TEM images (Figure 7). The inset in Figure 8 presents the pore size distribution curves calculated from the adsorption and desorption branches. Both curves show broad pore size distributions from about 10 to 100 nm, with peaks at 43.7 and 31.2 nm, respectively, belonging to mesopores. The sample also contains micropores

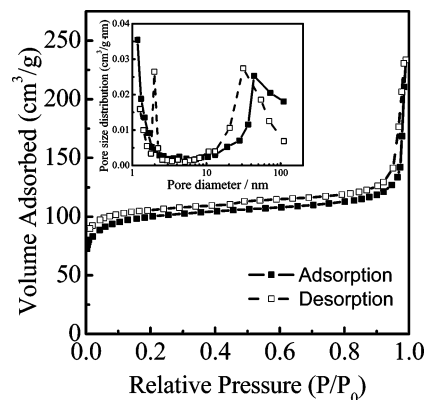


Figure 8. The nitrogen adsorption and desorption isotherms measured at 77 K for the carbonized electrospun fibers.

with diameters below 2 nm. The BET specific surface area and total pore volume of the samples are calculated to be 321.1 m²/g and 0.36 cm³/g, respectively. The micropore volume and mesopore volume were calculated to be 0.14 and 0.22 cm³/g, respectively, according to a modified standard adsorption plot (β_s plot).³¹

Discussion

The weight of the carbonized fibers was measured to be about 14.6 wt % of that of the pristine electrospun fibers. Apparent volume shrinkage has been observed after the fibers were oxidized, and one can also observe in the SEM images that the fibers stack more closely after oxidation and carbonization. However, as aforementioned, the average fiber diameter is about 500 nm for the pristine and the oxidized electrospun fibers, while it is about 600 nm for the carbonized fibers. It is noteworthy that, despite the serious mass loss, the fiber dimensions do not decrease largely

(31) Lukens, W. W.; Schmidt-Winkel, P.; Zhao, D. Y.; Feng, J. L.; Stucky, G. D. *Langmuir* **1999**, *15*, 5403.

but increase lightly after the oxidation and carbonization processes. Also, the pore size of carbonized fibers is somewhat larger than the domain size of the pristine fibers. Numerous studies have shown²⁷ that the degree of polymer orientation in PAN fibers decreases during heat-treatment, so tension needs to be applied to limit the thermal relaxation and improve the mechanical properties and thermal conductivity of final carbon fibers. As to our electrospun fibers, no tension has been applied during heat treatment, because our purpose is to prepare porous carbon fibers instead of high strength/modulus carbon fibers. The increase of fiber diameter after oxidation and carbonization processes may be related to the thermal relaxation of PAN macromolecules and a preferential shrinkage along the longitudinal axis of the fibers. Quantitative measurements are necessary in the future to illuminate the influence of heat treatment on fiber orientation and the influence of applied tension on the fiber morphologies during heat treatment.

The spin-casting PAN/poly(AN-*co*-MMA) film exhibited an interconnected phase structure with an average domain size of about 2 μm as aforementioned, which is much larger than the pore size in electrospun fibers. This apparently results from their differences in phase separation kinetics and influence of the strong elongation flow in electrospinning. The spin-casting film is much thicker and DMF evaporates relatively slowly, so the phase-separated domains have enough time to grow gradually to several micrometers. As to electrospinning, previous studies have demonstrated that the deposition rate of fibers during electrospinning is in the order of several tens of meters per second, the solution jet was elongated up to 10^5 times in less than a second, and the elongation rate can reach up to 10^4 s^{-1} , which leads to a dramatic increase of the surface-area-to-volume ratio within milliseconds.^{21,23} Because of the small diameter and large specific surface area of the electrospun fibers, the organic solvent in the sample solution evaporates rapidly during electrospinning and thus macroscopic phase separation is prevented. The orientation of pores along the longitudinal direction of the electrospun fibers is attributed to the rapid stretching effect during electrospinning.^{23,32} For example, carbon nanotubes embedded in electrospun fibers are always oriented along the fiber axis.^{16–18} Moreover, both theoretical and experimental investigations have demonstrated that strong shear and/or elongation flows cause the orientation of macromolecule chains along the direction of applied force and an anisotropic morphology of phase domains in many polymer mixtures.³³ We stress that no shear or elongation rates in previous experiments utilizing either the Poiseuille or the Couette flow are comparable to that in electrospinning.

(32) Wang, M.; Yu, J. H.; Kaplan, D. L.; Rutledge, G. C. P. *Macromolecules* **2006**, *39*, 1102.

(33) (a) Kim, Y. H.; Okamoto, M.; Kotaka, T.; Ougizawa, T.; Tchiba, T.; Inoue, T. *Polymer* **2000**, *41*, 4747. (b) Murase, H.; Kume, T.; Hashimoto, T.; Ohta, Y. *Macromolecules* **2005**, *38*, 6656. (c) Murase, H.; Kume, T.; Hashimoto, T.; Ohta, Y. *Macromolecules* **2005**, *38*, 8719.

It is also worth mentioning that, in comparison with the porous electrospun fibers prepared from highly volatile solvents, whose diameters are above 1 μm and pores exist only on the fiber surface, the nanoporous carbon fibers obtained in this study are much thinner and have continuous nanopores throughout the fiber surface and interior. Also, the porous fibers obtained by electrospinning a PLA/PVP/DCM ternary mixture followed by selectively removing one of the two polymers have a mean diameter of about 1–3 μm and a pore size of about 100 nm;²³ in contrast, we have prepared fibers with submicrometer diameters and nanopores of several tens of nanometers. Also, more important, the nanoporous structure survives after the oxidation and carbonization processes. Many electrospinning parameters and solution properties (e.g., molecular weight of the polymers, viscosity, conductivity, etc.) are responsible for these differences, while the role of solvent volatility should be especially emphasized. As compared to those highly volatile solvents employed in the literature, DMF in this study evaporates much less rapidly, allowing the solution jets to be stretched more sufficiently, leading to thinner fiber diameters and smaller phase domain sizes. Further systematic investigations should be conducted to take into consideration the influence of the compositions of both the polymer blends and the copolymer as well as the electrospinning factors on the morphology of nanoporous electrospun fibers. In general, by combination of electrospinning and microphase separation, we have prepared nanoporous submicrometer carbon fibers that are promising to be widely used in adsorption or filtration-related processes or as templates for preparing other nanostructured materials.

Conclusions

Ultrathin carbon fibers with an anisotropically elongated nanoporous structure have been obtained by electrospinning a mixture of PAN and poly(AN-*co*-MMA) in DMF followed by oxidizing and carbonizing the fibers. Because of the rapid solvent evaporation and solidification of the electrospun fibers during electrospinning, domain coarsening was limited, leading to fine and stretched phase domains. In the course of oxidation, the pyrolysis of the copolymer domains resulted in a porous structure in the fibers, which could be preserved after carbonization. Thus, ultrathin carbon fibers with a large amount of nanopores throughout the surface and the interior of the fibers were obtained. The nanopores in the fibers at about several tens of nanometers in widths are continuous. We believe the nanoporous carbon fiber obtained in this study has great potential for many applications.

Acknowledgment. We appreciate financial support from the National Natural Science Foundation of China (grant no. 50203013 and no. 20574060) and the Science & Technology Department of Zhejiang Province of China (Grant no. 200C21049).

LA061154G